

A Model for Sequential Threading of α -Cyclodextrin onto a Guest: A Complete Thermodynamic and Kinetic Study in Water

Christophe Saudan,[†] Frank A. Dunand,[†] Amira Abou-Hamdan,[†] Pascal Bugnon,[†] Peter G. Lye,[†] Stephen F. Lincoln,^{†,‡} and André E. Merbach^{*,†}

Contribution from the Institut de Chimie Minérale et Analytique, Université de Lausanne, CH-1015 Lausanne, Switzerland, and the Department of Chemistry, University of Adelaide, Adelaide SA 5005, Australia

Received April 12, 2001. Revised Manuscript Received July 26, 2001

Abstract: The first variable-temperature and variable-pressure stopped-flow spectrophotometric study of the sequential threading of α -cyclodextrin (α -CD) onto the guest dye Mordant Orange 10, **S**, is reported. Complementary ¹H one-dimensional (1D) variable-temperature kinetic studies and two-dimensional (2D) rotating-frame nuclear Overhauser effect spectroscopy (ROESY) and EXSY NMR studies are also reported. In aqueous solution at 298.2 K, the first α -CD threads onto **S** to form a 1:1 complex **S**· α -CD* with a forward rate constant $k_{1,f} = 15\,200 \pm 200 \text{ M}^{-1} \text{ s}^{-1}$ and dethreads with a reverse rate constant $k_{1,r} = 4.4 \pm 0.3 \text{ s}^{-1}$. Subsequently, **S**· α -CD* isomerizes to **S**· α -CD ($k_{3,f} = 0.158 \pm 0.006 \text{ s}^{-1}$, $k_{3,r} = 0.148 \pm 0.006 \text{ s}^{-1}$). This process can be viewed as a thermodynamically controlled molecular shuttle. A second α -CD threads onto **S**· α -CD* to form a 1:2 complex, **S**·(α -CD)₂*, with $k_{2,f} = 98 \pm 2 \text{ M}^{-1} \text{ s}^{-1}$ and $k_{2,r} = 0.032 \pm 0.002 \text{ s}^{-1}$. A second α -CD also threads onto **S**· α -CD to form another 1:2 complex, **S**·(α -CD)₂, characterized by $k_{4,f} = 9640 \pm 1800 \text{ M}^{-1} \text{ s}^{-1}$ and $k_{4,r} = 61 \pm 6 \text{ s}^{-1}$. Direct interconversion between **S**·(α -CD)₂* and **S**·(α -CD)₂ was not detected; instead, they interconvert by dethreading the second α -CD and through the isomerization equilibrium between **S**· α -CD* and **S**· α -CD. The reaction volumes, ΔV^{\ddagger} , were found to be negative for the first three equilibria and positive for the fourth equilibrium. For the first three forward and reverse reactions, the volumes of activation are substantially more negative, indicating a compression of the transition state in comparison with the ground states. These data were used in conjunction with ΔH^{\ddagger} , ΔH° , ΔS^{\ddagger} , and ΔS° data to deduce the dominant mechanistic threading processes, which appear to be largely controlled by changes in hydration and van der Waals interactions, and possibly by conformational changes in both **S** and α -CD. The structure of the four complexes were deduced from ¹H 2D ROESY NMR studies.

Introduction

Naturally occurring α -cyclodextrin (α -CD) is a six-membered α -1,4-linked cyclic oligomer of D-glucopyranose and is generally described as a shallow truncated cone, with the primary hydroxy rim of the cavity having a reduced diameter compared to the secondary hydroxy rim. The interior of the cavity is lined by methylene and methine hydrogen atoms and ether oxygens and as a consequence is hydrophobic. Because of this and its constrained size, the cyclodextrin cavity selectively complexes guest molecules in aqueous solution.¹ The driving force for the complexation is the sum of weak secondary interactions for which the thermodynamic parameters are often not readily interpreted. The principal factors involved in the stability of these noncovalent host–guest inclusion complexes are believed to be primarily hydrophobic and van der Waals interactions,¹ although the relief of cyclodextrin strain energy² and the release of partially hydrogen-bonded activated water molecules from the cavity³ are thought to have a role also. To achieve a predictive capability for the inclusion process and full mechanistic understanding, it is well accepted⁴ that kinetic studies on

a wide range of substrates have to be performed. However, in the past decades, the transition states of the inclusion reactions involving α -CD have been characterized experimentally by the evaluation of the activation parameters ΔH^{\ddagger} and ΔS^{\ddagger} , which are usually not simple to interpret on the molecular level.⁵

Recently, we have undertaken a variable-pressure kinetic study together with a classical variable-temperature investigation of the formation of 1:1 complexes formed through the inclusion of a series of diphenylazo dyes by α -CD.⁶ The guest dye molecules were selected to favor a directionality in the inclusion process and to systematically tune steric and electronic effects toward molecular recognition of the guest by the α -CD host. For the first time, activation volumes were obtained for inclusion reactions where a guest species was included in the α -CD cavity and revealed characteristic trends depending on the substituent groups of the dyes. The activation and reaction volumes were interpreted in the context of other thermodynamic and kinetic data for the complex formation in order to construct a global view of the inclusion process.

The formation of pseudopolyrotaxanes based on α -CD, which result from the threading⁷ of several α -CD rings onto a linear

* Corresponding author: e-mail andre.merbach@icma.unil.ch.

[†] Université de Lausanne.

[‡] University of Adelaide.

(1) Rekharsky, M. V.; Inoue, Y. *Chem. Rev.* **1998**, *98*, 1875.

(2) Manor, P. C.; Saenger, W. J. *J. Am. Chem. Soc.* **1974**, *96*, 3690.

(3) Griffiths, D. W.; Bender, M. L. *Adv. Catal.* **1973**, *23*, 209.

(4) Connors, K. A. *Chem. Rev.* **1997**, *97*, 1325.

(5) (a) Yoshida, N.; Seiyama, A.; Fujimoto, M. *J. Phys. Chem.* **1990**, *94*, 4246. (b) Hersey, A.; Robinson, B. H. *J. Chem. Soc., Faraday Trans. 1* **1984**, *80*, 2039. (c) Seiyama, A.; Yoshida, N.; Fujimoto, M. *Chem. Lett.* **1985**, 1013. (d) Yoshida, N. *J. Chem. Soc., Perkin Trans. 2* **1995**, 2249. (6) Abou-Hamdan, A.; Bugnon, P.; Saudan, C.; Lye, P. G.; Merbach, A. E. *J. Am. Chem. Soc.* **2000**, *122*, 592.

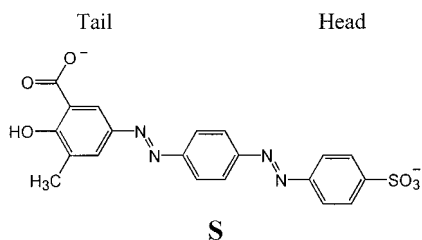


Figure 1. Molecular structure of guest S.

polymeric guest, has attracted recent attention.^{8,9} Most of the polymeric pseudorotaxanes reported in the literature¹⁰ exhibit very low solubility in aqueous solution and hence kinetic investigations of the threading process are limited.¹¹ In the work presented here, we focus on the successive threading in water of two α -CDs onto a dye S, bearing a sulfonate head as the inserting group and a bulky stopper at the tail (Figure 1). The structure of the guest dye, differing only from the previously⁶ studied diphenylazo dye by an additional diazophenyl moiety in the hydrophobic core, was selected to both control the direction of threading and to be a sufficient length to accommodate two α -CDs. The energetic characteristics of the threading processes, leading to the formation of four different complexes, were determined from NMR measurements together with kinetic investigations with pressure and temperature as experimental variables. It will be seen that in this system we observe the operation of a simple thermodynamically controlled molecular shuttle; such systems are attracting increasing interest as potential molecular switches for nanotechnology application.^{12,13}

Experimental Section

Materials. The azo guest molecule S (Mordant Orange 10) was purchased from Aldrich and purified by column chromatography as described elsewhere.^{5a} α -CD purchased from Fluka was used without further purification. Both the dye and uncharged α -CD solutions were prepared in doubly distilled water.

Spectrophotometric Measurements. All measurements were carried out at 298.2 ± 0.1 K with the ionic strength, I , fixed to 0.15 M (NaCl). The acid dissociation constant, K_a , of the dye was determined by a combination of potentiometric and spectrophotometric techniques. The instrumentation used consists of a titroprocessor (Titrimo 716 from Metrohm) for the addition of titrant and millivolt readings and of a diode-array spectrometer (TIDAS-MMS-UV/500-1 from J&M) coupled to a Hellma immersion probe (10 mm path length) for the spectrophotometric measurements. A combined glass electrode (Metrohm) was calibrated from a titration of a known amount of HCl in water with a known concentration of NaOH. The pH values are defined as $-\log [H^+]$. The aqueous solution of the dye S (5×10^{-5} M, basified with Na₃PO₄), was titrated under argon with 0.1 M HCl from pH 12 to 3.5. The solution was thoroughly mixed and allowed to equilibrate before the spectrum was acquired directly with the immersion probe present inside the titration vessel. The pK_a value of the dye was calculated by use of the fitting software SPECFIT.¹⁴

Stopped-Flow Kinetic Experiments. Both the dye [(1.5–5.0) $\times 10^{-5}$ M] and uncharged α -CD [(0.3–10) $\times 10^{-3}$ M] were dissolved in doubly distilled water without the addition of an electrolyte. The kinetics

(7) When the guest species is longer than the central axis of the α -CD host, the latter may be viewed as “threaded” onto the former, and to be in accord with the current usage we have adopted the term “threading” in place of “inclusion”.

(8) Harada, A.; Kamachi, M. *Macromolecules* **1990**, *23*, 2821.

(9) Wenz, G.; Keller, B. *Angew. Chem., Int. Ed. Engl.* **1992**, *31*, 197.

(10) Nepogodiev, S. A.; Stoddart, J. F. *Chem. Rev.* **1998**, *98*, 1959 and references therein.

(11) Herrmann, W.; Keller, B.; Wenz, G. *Macromolecules* **1997**, *30*, 4966.

(12) Bissell, R. A.; Córdova, E.; Kaifer, A. E.; Stoddart, J. F. *Nature* **1994**, *369*, 133.

of the threading reaction between the dye and α -CD were investigated by the stopped-flow technique in the absorption mode for detection. In addition, these experiments were performed under pseudo-first-order conditions in the presence of at least a 10-fold excess of α -CD. Temperature-dependent kinetic measurements were carried out between 274 and 318 K on an Applied Photophysics SX.18MV stopped-flow spectrometer. Pressure-dependent kinetic measurements were made up to 200 MPa by use of high-pressure stopped-flow equipment designed and built in-house.¹⁵ The rate constants were independent of the sequence of applied pressure. For both temperature and pressure kinetic measurements, a J&M TIDAS diode array spectrometer was used for detection when reaction time allowed it. In other cases, the temperature and pressure dependencies of the reaction were monitored at discrete wavelengths from 350 to 500 nm on the monowavelength detection system and the acquisition facility provided with the Applied Photophysics SX.18MV stopped-flow spectrometer. For each set of experimental conditions, a series of four to six replicate data sets were averaged. For both the temperature and pressure multiwavelength experiments, the observed rate constants were computed via an iterative procedure where exponential functions were fitted to the absorbance/time data by use of global analysis software.^{14,16} Reported errors are 1 standard deviation.

NMR Measurements. ¹H NMR experiments were recorded on Bruker DPX 400 (400 MHz) and DRX 600 (600 MHz) spectrometers with the samples nonspinning. All NMR experiments (dye titration by α -CD, differential NOE, dilution experiments, etc.) were carried out in D₂O with sodium 2,2-dimethyl-2-silapentane-5-sulfonate (DSS, Fluka) as an external standard. For all experiments, the temperature was stabilized by Bruker VT-2000 and BVT-3000 temperature control units and measured by a substitution method.¹⁷

The dye self-association (π - π stacking) was determined by ¹H NMR dilution experiments at 298.2 K. The dye concentration was varied from 1.0×10^{-4} to 1.0×10^{-2} M and the induced chemical shift changes were analyzed with the program Scientist¹⁸ using the relevant equations.⁶ The stability constants were obtained from NMR spectral measurements at 274.2 K with a solution of dye S (9.40×10^{-4} M) in D₂O (pD ca. 6.5) titrated with consecutive additions of solid α -CD. The resulting solutions were thoroughly mixed and allowed to equilibrate for at least 10 min before the spectrum was acquired. The ratio of the total α -CD concentration to the total dye concentration of 9.40×10^{-4} M was varied between 0 and 42. The NMR signals were fitted by Lorentzian functions with the program NMRICMA.¹⁹ NMR dynamic processes were quantitatively determined by variable temperature measurements for a solution containing 0.0168 M α -CD and 9.13×10^{-3} M S. Rate constants were obtained from line-broadened NMR spectra by least-squares fitting with the program NMRICMA¹⁹ using the appropriate exchange matrix. Fast injection experiments were performed at 278.2 K with a fast-injection apparatus described elsewhere.²⁰

All 2D NMR experiments (DQF-COSY, EXSY, ROESY) were acquired from 1024 increments of 2 K data points and 16 scans each. The data were zero-filled twice in the t_1 dimension and multiplied by a squared sine bell function (SSB) in both dimensions. NMR spectroscopic data processing was carried out on a Bruker Silicon

(13) Brouwer, A. M.; Frochet, C.; Gatti, F. G.; Leigh, D. A.; Mottier, L.; Paolucci, F.; Roffia, S.; Wurpel, G. W. H. *Science* **2001**, *291*, 2124.

(14) SPECFIT 2.11 for MS-DOS, Spectrum Software Associates, P.O. Box 4494, Chapel Hill, NC 27515; e-mail SpecSoft@compuserve.com.

(15) Bugnon, P.; Laurenczy, G.; Ducommun, Y.; Sauvageat, P.-Y.; Merbach, A. E.; Ith, R.; Tschanz, R.; Doludra, M.; Bergbauer, R.; Grell, E. *Anal. Chem.* **1996**, *68*, 3045.

(16) (a) Gampp, H.; Maeder, M.; Meyer, C. J.; Zuberbühler, A. D. *Talanta* **1985**, *32*, 95. (b) Gampp, H.; Maeder, M.; Meyer, C. J.; Zuberbühler, A. D. *Talanta* **1985**, *32*, 257. (c) Gampp, H.; Maeder, M.; Meyer, C. J.; Zuberbühler, A. D. *Talanta* **1985**, *32*, 1133. (d) Gampp, H.; Maeder, M.; Meyer, C. J.; Zuberbühler, A. D. *Talanta* **1986**, *33*, 943.

(17) Ammann, C.; Meier, P.; Merbach, A. E. *J. Magn. Reson.* **1982**, *46*, 319.

(18) Scientist 2.0; MicroMath, Inc.: Salt Lake City, UT, 1995.

(19) Helm, L.; Borel, A. NMRICMA 2.03; Lausanne University: Lausanne, Switzerland, 1998.

(20) Bernhard, P.; Helm, L.; Ludi, A.; Merbach, A. E. *J. Am. Chem. Soc.* **1985**, *107*, 312.

Graphics O2 station with standard UXNMR software as well as on a PC with 1D WIN NMR (960901) software (Bruker Franzen Analytic GmbH).

Results

Equilibrium and Structural Aspects. All the equilibrium and kinetic measurements were carried out in pure water (pH around 6.5) because it is known that electrolyte ions also form complexes with cyclodextrins.²¹ It was thus essential to study the protonation behavior of the dye and determine the existing species under such conditions. From the titration of the dye at 298 K in the pH range of 12–3.5, an acid dissociation constant (pK_a) of 11.51 ± 0.01 was obtained. On the basis of our previous study⁶ with similar molecules, this value may be unambiguously attributed to the pK_a of the phenolic group of the dye. At lower pH, we have observed the precipitation of **S**, which is probably a consequence of the protonation of the carboxylate group. Therefore, it is estimated that the pK_a of the carboxylic acid group is about 2.5, which is consistent with other studies.⁶ Accordingly, it may be assumed that in pure water the dye exists predominantly in the form that is shown in Figure 1. It is worth noting that the values of the acid dissociation constants (pK_a) of the guest may be enhanced upon complexation in cyclodextrins,²² so that changes in the extent of protonation of the guest can occur. However, for complexation reactions with α -CD a negligibly small increase of the pK_a was observed for guest species similar to that studied here.²³ On this basis, the extent of protonation is unlikely to be affected by complexation by α -CD under the experimental conditions employed.

In the case of the diphenylazo dyes it was demonstrated⁶ that a π - π stacking-driven self-association leading to dimerization occurs in aqueous solution and that this effect can be clearly observed by chemical shift changes upon dilution. By methods similar to those in our previous study⁶ with a series of diphenylazo dyes, ¹H NMR dilution experiments were performed and the chemical shift changes were fitted as a function of the total dye concentration by use of a model describing the formation of the dimer (**S**₂). An association constant of $K_{\text{assoc}} = 187 \pm 4 \text{ M}^{-1}$ was determined from the NMR analysis (fits are given in Supporting Information) and the geometry of dimerization is an antiparallel orientation of two **S** dye molecules, as confirmed by differential nuclear Overhauser effects (NOE). This value is about 10 times larger than the order of magnitude of the diphenylazo dye association constants.⁶ In the present study, the higher stability of the dimeric form of **S** probably arises from the additional diazophenyl group producing a stronger π - π interaction. Since we are working at dye concentrations of $(1.5\text{--}5.0) \times 10^{-5} \text{ M}$ for the stopped-flow kinetic studies, the presence of the dimeric species can be neglected as it accounts for less than 2.0% of the total dye concentration.

To determine the stability constants of the species formed upon threading of α -CD by **S**, a 1D ¹H NMR titration at 274.2 K was performed. For that purpose, the magnetic environment of the dye methyl group was selected in order to better visualize the spectral evolution. The titration of **S** with α -CD, which is shown in Figure 2, resulted in the appearance of four complexes: **S**· α -CD*, **S**· α -CD, **S**·(α -CD)₂*, and **S**·(α -CD)₂. Strikingly, the chemical shift of free **S** varies with the α -CD concentration. As previously described,⁶ this effect is due to

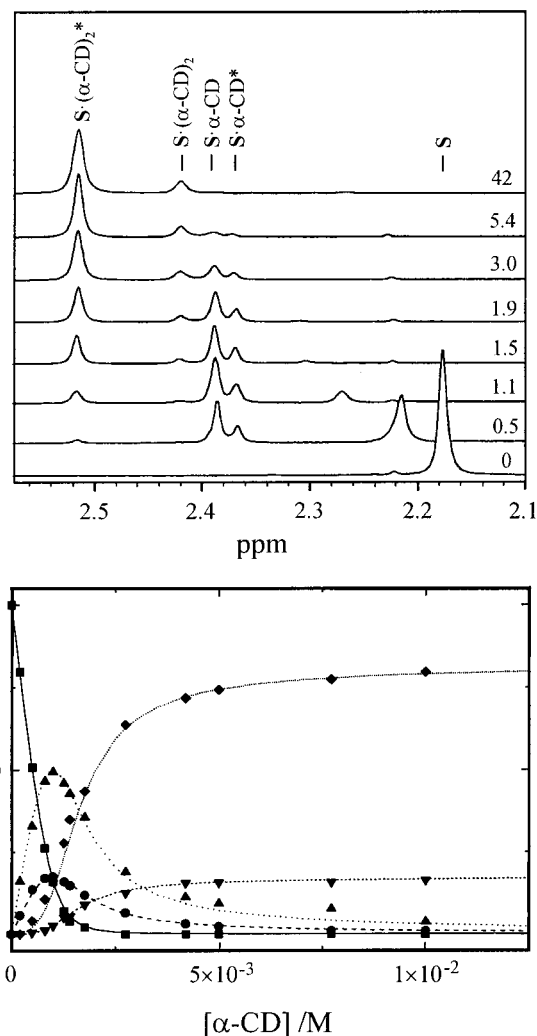


Figure 2. ¹H NMR (400 MHz) titration of **S** with α -CD in D₂O at 274.2 K, pD ca. 7. The upper panel shows the spectral evolution of the **S** methyl resonances corresponding to the different species formed by increasing the α -CD concentration. On the right of each spectrum lies the ratio of the α -CD concentration to the total **S** concentration of $9.30 \times 10^{-4} \text{ M}$. The lower panel shows the percentage of the species **S** (■), **S**· α -CD* (●), **S**· α -CD (▲), **S**·(α -CD)₂ (▼), and **S**·(α -CD)₂* (◆) as a function of the α -CD concentration. The lines represent the fit of the points according to the model presented in Figure 5.

the π - π stacking-driven self-association of **S**. This dimerization is a fast process on the NMR time scale since only an average set of signals for **S** and **S**₂ is observed. In contrast, the α -CD threading process at low temperature is much slower as indicated by the presence of separate sets of NMR signals for the complexed forms. At 298.2 K, the coalescence of the signals corresponding to **S**· α -CD and **S**·(α -CD)₂* has already occurred. In Figure 2, the plots of the signal integrals of the species as a function of α -CD concentration shows that states **S**· α -CD and **S**· α -CD* are formed at low concentration and a higher stability is exhibited by **S**· α -CD compared with **S**· α -CD*. These species are likely to have similar structures to those 1:1 complexes reported for a series of diphenylazo dyes having a sulfonate head.⁶ At higher concentrations of α -CD, only the complexes **S**·(α -CD)₂ and **S**·(α -CD)₂* are detected. Under these conditions, both complexes exist in a constant ratio of 82% **S**·(α -CD)₂* coexisting with 18% **S**·(α -CD)₂, consistent with these complexes both possessing 1:2 stoichiometry as is further discussed below.

(21) Rohrbach, R. P.; Rodriguez, L. J.; Eyring, E. M.; Wojcik, J. F. *J. Phys. Chem.* **1977**, *81*, 944.

(22) Connors, K. A.; Lipari, J. M. *J. Pharm. Sci.* **1976**, *65*, 379.

(23) Yoshida, N.; Seiyama, A.; Fujimoto, M. *J. Phys. Chem.* **1990**, *94*, 4254.

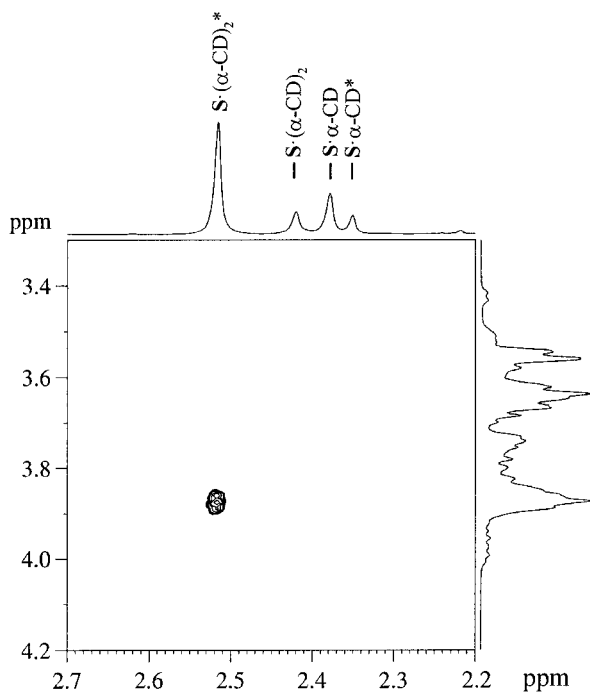


Figure 3. ^1H 2D-ROESY NMR (600 MHz) spectrum of a mixture of **S** (9.07×10^{-3} M) and α -CD (0.0158 M) in D_2O recorded at 274.2 K using a spin-lock time of 300 ms. This 2D spectrum shows an intermolecular ROE for the **S** methyl group of $\text{S}\cdot(\alpha\text{-CD})_2^*$ with the H(3) inner protons of the first threaded α -CD, only.

It is known that rotating-frame nuclear Overhauser effect spectroscopy (ROESY) experiments provide detailed information on the proximity of host and guest molecules.^{24,25} Figure 3 shows an intermolecular ROE cross-peak between the guest methyl protons and the H(3) inner proton of the α -CD for the $\text{S}\cdot(\alpha\text{-CD})_2^*$ complex and the absence of this interaction for the other complexes. On the basis of this result, we can conclude that one α -CD of complex $\text{S}\cdot(\alpha\text{-CD})_2^*$ is threaded with its wide rim close to the tail of **S** as a ROE interaction occurs between the α -CD H(3) proton and the methyl group. To determine the structure of this complex, we prepared a mixture containing **S** and an excess of α -CD in order to detect only species $\text{S}\cdot(\alpha\text{-CD})_2$ and $\text{S}\cdot(\alpha\text{-CD})_2^*$ in solution. From NOEDIF, 2D double-quantum-filtered correlation spectroscopy (DQF-COSY), and ROESY techniques, a complex geometry for $\text{S}\cdot(\alpha\text{-CD})_2^*$ was deduced (see Supporting Information). It emerged from these experiments that **S** threads two α -CDs, which adopt a head-to-tail orientation.

Kinetic and Mechanistic Aspects. Cyclodextrin host–guest complexes exist in dynamic equilibrium with their free cyclodextrin host and guest components.^{6,26,27} For the study of host–guest exchange processes in such systems, 2D EXSY NMR spectroscopy is an ideal technique^{28,29} and was applied in our case to address some features of the threading reaction mechanism. Figure 4 illustrates the successive dynamic equilibria between the **S**, $\text{S}\cdot\alpha\text{-CD}^*$, and $\text{S}\cdot(\alpha\text{-CD})_2^*$ states. Since $\text{S}\cdot(\alpha\text{-CD})_2^*$ is a 1:2 complex, we deduce that the free **S** forms the $\text{S}\cdot(\alpha\text{-CD})_2^*$ complex by successive threadings of two α -CD via the 1:1 complex $\text{S}\cdot\alpha\text{-CD}^*$. In Figure 4, successive dynamic equilibria between the $\text{S}\cdot\alpha\text{-CD}^*$, $\text{S}\cdot\alpha\text{-CD}$, and $\text{S}\cdot(\alpha\text{-CD})_2^*$ states are also shown to occur. Thus, the complex $\text{S}\cdot\alpha\text{-CD}^*$ isomerizes to a second intermediate complex $\text{S}\cdot\alpha\text{-CD}$, as was observed with the diphenylazo dyes, and subsequently forms the 1:2 complex $\text{S}\cdot(\alpha\text{-CD})_2$. On the basis of these results, we postulate the reaction mechanism presented in Figure 5, which accounts for the formation pathways of the 1:2 complexes $\text{S}\cdot(\alpha\text{-CD})_2$ and $\text{S}\cdot(\alpha\text{-CD})_2^*$ in aqueous solution. Other experimental observations support the validity of this mechanism and the geometry of the complexes as is discussed below.

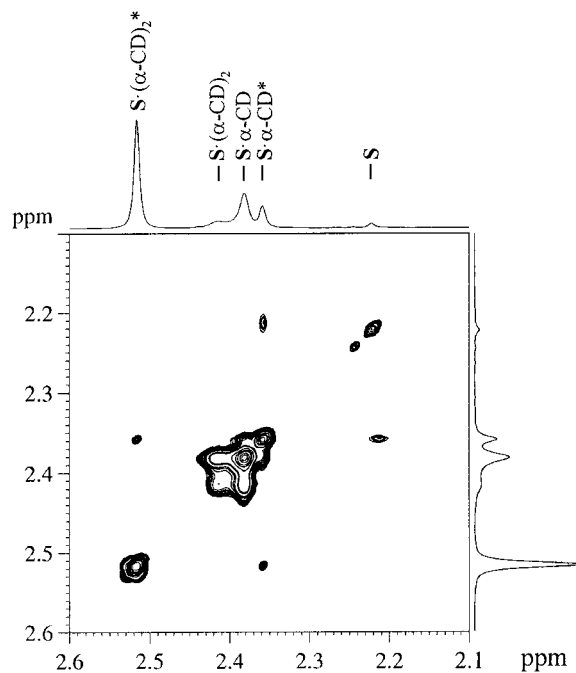


Figure 4. ^1H 2D-EXSY NMR (400 MHz) spectrum of a mixture of **S** (9.07×10^{-3} M) and α -CD (0.0158 M) in D_2O recorded at 291.2 K with a mixing time of 300 ms. This spectrum shows clearly the existing exchanges between the different species.

To follow the evolution of the complexation process as a function of time and to discriminate qualitatively between the slow and the fast kinetic processes, an NMR fast injection experiment was performed over 50 s by mixing 0.470 g of 5.88×10^{-2} M α -CD solution with 2.099 g of a 6.60×10^{-3} M solution of **S**. The result of this experiment, which is shown in Supporting Information, demonstrates that the threading of α -CD by **S** to form $\text{S}\cdot\alpha\text{-CD}^*$ is fast and that the isomerization of $\text{S}\cdot\alpha\text{-CD}^*$ and the formation of the complex $\text{S}\cdot(\alpha\text{-CD})_2^*$ from $\text{S}\cdot\alpha\text{-CD}^*$ are comparatively slow. These deductions accord with those derived from the 2D EXSY NMR spectrum (see Figure 4) and identify the role of $\text{S}\cdot\alpha\text{-CD}^*$ in the reaction pathway.

Reaction kinetics were quantitatively determined by the stopped-flow technique in the absorption mode for detection and were analyzed according to eqs 1–3 discussed below. Prior to measurement of the threading of α -CD by **S** under different conditions, the photostability of **S** and S/α -CD mixtures were investigated. It is well-known that UV–visible irradiation of the azobenzene moiety can cause cis–trans isomerization,³⁰ to the extent that Nakashima et al. used this photophysical property to prepare an α -CD-based photoswitchable [2]-rotaxane.³¹ In

(24) Ikeda, H.; Nakamura, M.; Isee, N.; Toda, F.; Ueno, A. *J. Org. Chem.* **1997**, *62*, 1411.

(25) Schneider, H.-J.; Hacket, F.; Rüdiger, V. *Chem. Rev.* **1998**, *98*, 1755.

(26) Cramer, F.; Saenger, W.; Spatz, H.-Ch. *J. Am. Chem. Soc.* **1967**, *89*, 14.

(27) Clarke, R. J.; Coates, J. H.; Lincoln, S. F. *J. Chem. Soc., Faraday Trans. 1* **1984**, *80*, 3119.

(28) Cai, M.; Sidorov, V.; Lam, Y.-F.; Flowers, R. A.; Davis, J. T. *Org. Lett.* **2000**, *2*, 1665.

(29) Brottin, T.; Lesage, A.; Emsley, L.; Collet, A. *J. Am. Chem. Soc.* **2000**, *122*, 1171.

(30) Rau, H. *Photochemistry and Photophysics*; Rabek, J. F., Ed.; CRC Press: Boca Raton, FL, 1990; Vol. 2, p 119.

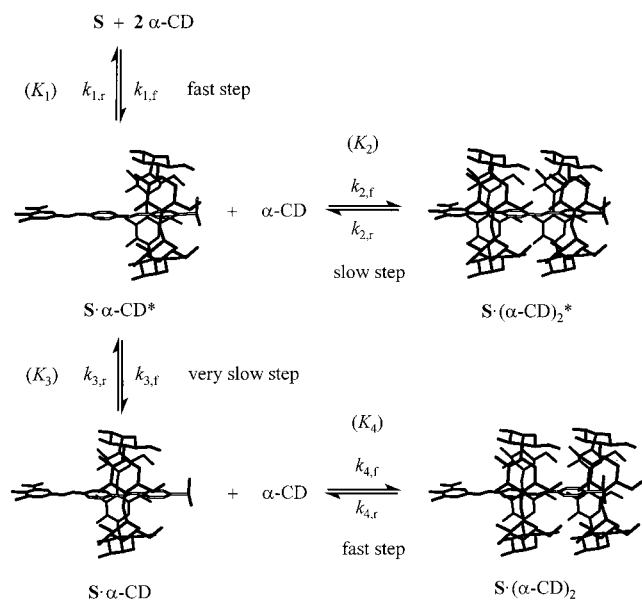


Figure 5. Mechanism for the threading reactions of **S** with α -CD. These proposed structures are based on 2D NMR data and employ dimensions similar to those observed in α -CD crystal structures and reported for **S** derived through modeling. A single arbitrarily chosen conformation is shown for α -CD in each complex and does not show the hydrogen-bonding interactions discussed in the text. All hydrogen atoms of the supramolecular structures are omitted for clarity.

our case, the absorbance of **S** and **S**/ α -CD mixtures was monitored over 10 min at different temperatures over a range of UV–visible wavelengths, and no absorbance change was observed. It was concluded that either cis–trans isomerizations of **S** are very slow processes under our experimental conditions or the cis isomers have extremely short half-lives and hence are not significantly populated.³²

The stopped-flow measurements showed that three steps were involved in the threading process, irrespective of the α -CD concentration, temperature, and pressure. An example of typical data is shown in Figure 6. In addition, it was verified that no very fast processes occur during the instrumental mixing time. The validity of the pseudo-first-order conditions was also checked by varying the dye concentration with a constant α -CD concentration (with at least a 10-fold excess of α -CD), and it was determined from these measurements that the complexation rates did not depend on **S** concentration. Figure 6 illustrates that a fast step precedes the two slower processes. To confirm that the slower processes did not arise from back-diffusion in the stopped-flow apparatus, they were also studied by conventional methods on a standard UV–visible spectrometer. The observed rate constants obtained by both methods were identical within experimental error. The observed rate constants for the first fast step, $k_{1,\text{obs}}$, and the slow second step, $k_{2,\text{obs}}$, show a linear dependence on the α -CD concentration. However, for the second step, a slight curvature is observed at very low α -CD concentration, because of the sequential nature of the complexation. From these results, it is apparent that the first and the second steps involve threading of α -CD by **S**, as observed in previous complexation studies of other guests by cyclodextrins.^{5a,6,26} The values of the observed rate constants for the third very slow isomerization step, $k_{3,\text{obs}}$, increase as a function of the α -CD concentration but reach a saturation value and then

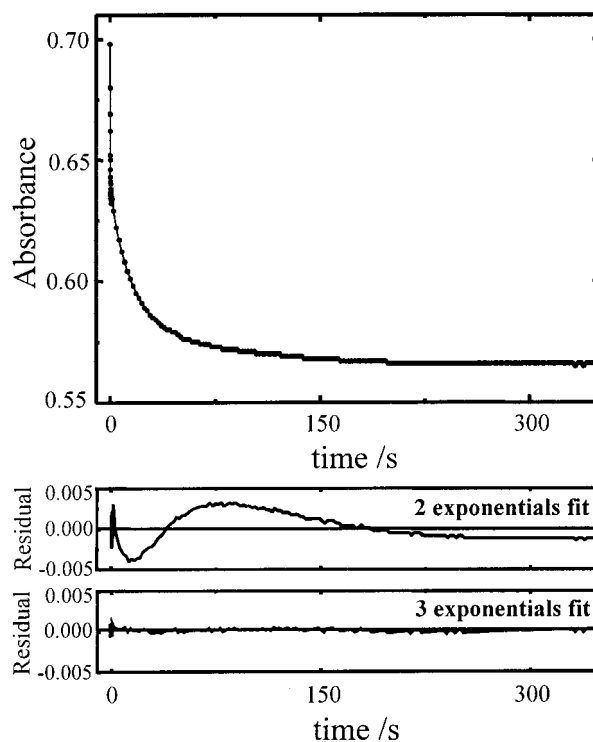


Figure 6. Kinetic trace at 375 nm of the threading reactions between **S** and α -CD at 278 K. $C_{\alpha\text{-CD}} = 0.74 \times 10^{-3}$ M, $C_{\text{S}} = 2.54 \times 10^{-5}$ M, $I = 0$ M. The residuals show clearly the necessity of a three-exponential function to fit the kinetic data. The observed rate constants and relative amplitudes for the sum of three exponentials for the reaction are as follows: $k_{1,\text{obs}} = 6.31 \text{ s}^{-1}$ and $A_1 = 0.54$; $k_{2,\text{obs}} = 0.072 \text{ s}^{-1}$ and $A_2 = 0.33$; $k_{3,\text{obs}} = 0.011 \text{ s}^{-1}$ and $A_3 = 0.13$.

decrease at higher concentrations of α -CD as predicted by eq 3 (Figure 7). In the case of diphenylazo dye complexation kinetics with α -CD, saturation-type concentration dependences of the observed rate constants were also attributed to an isomerization process.^{5a,b,6}

The reaction scheme given in Figure 5 accommodates the experimental observations, where the first fast step and the second slow step originate, respectively, from the threading of α -CD by **S** to give the $S\alpha\text{-CD}^*$ complex and from the threading of an additional α -CD by $S\alpha\text{-CD}^*$, leading to the formation of the 1:2 complex $S(\alpha\text{-CD})_2^*$. As mentioned above, the third very slow step arises from an isomerization process of the intermediate $S\alpha\text{-CD}^*$ to $S\alpha\text{-CD}$, which subsequently threads another α -CD to give $S(\alpha\text{-CD})_2$ at high α -CD concentration. These observations from stopped-flow experiments are in accord with the fast-injection NMR experiments described above. Surprisingly, the formation of the 1:2 complex $S(\alpha\text{-CD})_2$ was not observed by stopped-flow measurements. It is possible that the spectra of $S\alpha\text{-CD}$ and $S(\alpha\text{-CD})_2$ do not differ greatly and consequently the latter species is not detected. Nevertheless, this process was identified by 2D EXSY NMR (Figure 4).

If the first and the fourth steps are fast compared to the other processes (see Figure 5), the observed rate constants may be expressed by eqs 1–3 (see Supporting Information for more details):

$$k_{1,\text{obs}}(\text{fast}) = k_{1,f}C_{\alpha\text{-CD}} + k_{1,r} \quad (1)$$

$$k_{2,\text{obs}}(\text{slow}) = \frac{1}{2}(p + \sqrt{p^2 - 4q}) \quad (2)$$

$$k_{3,\text{obs}}(\text{very slow}) = \frac{1}{2}(p - \sqrt{p^2 - 4q}) \quad (3)$$

(31) Murakami, H.; Kawabuchi, A.; Kotoo, K.; Kunitake, M.; Nakashima, N. *J. Am. Chem. Soc.* **1997**, *119*, 7605.

(32) Irick, G., Jr.; Pacifici, J. G. *Tetrahedron Lett.* **1969**, 1303.

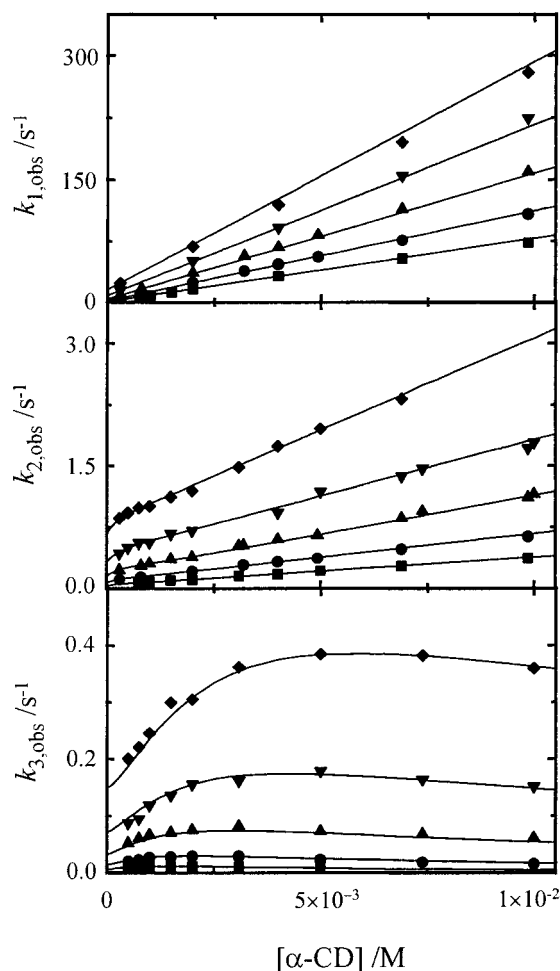


Figure 7. Temperature dependence of $k_{1,obs}$, $k_{2,obs}$, and $k_{3,obs}$ for the threading of α -CD by **S**: $C_S = (1.5\text{--}5.0) \times 10^{-5}$ M, $I = 0$ M, and $T = 278$ (■), 288 (●), 298 (▲), 308 (▼), or 318 (◆) K.

where

$$p = \frac{k_{3,r}}{1 + K_4 C_{\alpha\text{-CD}}} + k_{2,r} + \frac{K_1 C_{\alpha\text{-CD}}}{1 + K_1 C_{\alpha\text{-CD}}} (k_{3,f} + k_{2,f} C_{\alpha\text{-CD}})$$

$$q = \frac{k_{3,r} k_{2,r}}{1 + K_4 C_{\alpha\text{-CD}}} + \frac{k_{3,r} k_{2,f} C_{\alpha\text{-CD}}}{1 + K_4 C_{\alpha\text{-CD}}} \left(\frac{K_1 C_{\alpha\text{-CD}}}{1 + K_1 C_{\alpha\text{-CD}}} \right) + \frac{K_1 C_{\alpha\text{-CD}}}{1 + K_1 C_{\alpha\text{-CD}}} (k_{3,f} + k_{2,r})$$

with $K_1 = k_{1,f}/k_{1,r}$ and $K_4 = k_{4,f}/k_{4,r}$.

The α -CD concentration dependences for the observed rate constants, $k_{1,obs}$, $k_{2,obs}$, and $k_{3,obs}$, which were obtained at various temperatures, were fitted simultaneously by use of eqs 1–4 with a procedure described elsewhere.⁶ The derived values are listed in Table 1 and the fit of the data is shown in Figure 7. The stability constants derived from the analysis of the NMR titration according to the proposed reaction scheme show a good agreement with those determined by stopped-flow kinetic measurements (see Table 1). These observations demonstrate the plausibility of the mechanistic scheme shown in Figure 5.

$$k = \frac{k_B T}{h} \exp\left(\frac{\Delta S^\ddagger}{R} - \frac{\Delta H^\ddagger}{RT}\right) \quad (4)$$

The pressure dependence of the observed rate constants were studied up to 200 MPa.³³ It emerged from these measurements

that both $\ln k_f$ and $\ln k_r$ for the three steps change linearly with pressure, indicating that the activation volumes are pressure-independent under our experimental conditions.³⁴ This enabled the pressure and the α -CD concentration dependences of the observed rate constants for all steps to be simultaneously fitted by use of eqs 1–3 and 5, where k_0 is the extrapolated rate constant at zero pressure and ΔV^\ddagger is the activation volume. The result of the simultaneous fit is shown in Figure 8 and activation volumes are presented in the volume profile depicted in Figure 9. At 288 K, the rate and the equilibrium constants extrapolated at zero pressure from the variable kinetic studies correlate very well with the one interpolated from the kinetic measurements at variable temperature (see Supporting Information).

$$k = k_0 \exp\left(-\frac{\Delta V^\ddagger P}{RT}\right) \quad (5)$$

To determine the rate constants $k_{4,f}$ and $k_{4,r}$, variable-temperature 1D NMR measurements were performed with the coalescence of the **S**· α -CD and **S**·(α -CD)₂ signals between 268 and 310 K in a solution containing 9.13×10^{-3} M dye **S** with 0.0168 M α -CD (see Supporting Information). Under these experimental conditions, no exchange phenomena were observed for the other complexation processes. Each spectrum was analyzed according to a two-site exchange with $k_{4,r}$ (in reciprocal seconds, s⁻¹) and the population ratio as parameters. The first-order process described by $k_{4,r}$ was confirmed by similar procedures at another concentration of α -CD. Since it was difficult to determine experimentally the concentration of the free α -CD, the second-order rate constant $k_{4,f}^{298}$ (in liters per mole per second, M⁻¹ s⁻¹) was estimated from $k_{4,r}^{298}$ determined by this NMR experiment and the stability constant, K_4^{298} (in liters per mole, M⁻¹), obtained by stopped-flow measurements. This estimation is valuable, in the sense that the stability constants obtained by NMR titration and those derived from kinetic measurements are consistent. The rate constants for the fourth step ($k_{4,f}^{298}$ and $k_{4,r}^{298}$) are reported in Table 1 and show that this process is fast. The enthalpy and entropy of activation, $\Delta H_{4,r}^\ddagger$ and $\Delta S_{4,r}^\ddagger$, are obtained from the fit of $k_{4,r}$ at different temperatures with eq 4, and the enthalpy and entropy of activation, $\Delta H_{4,f}^\ddagger$ and $\Delta S_{4,f}^\ddagger$, are derived from the reaction parameters determined by the stopped-flow measurements. In conclusion, this experiment provides an additional observation of the exchange between species **S**· α -CD and **S**·(α -CD)₂ to that obtained from the EXSY experiments (see Figure 3).

Discussion

The mechanism proposed for the threading of one and two α -CD onto the dye, **S**, to form four distinct complexes, whose structures are based on the NMR studies and on previous⁶ modeling of related systems, is depicted in Figure 5. The rate and the associated equilibrium constants (as defined in Figure 5) and thermodynamic parameters are collected in Table 1, and the accompanying volume profiles are shown in Figure 9. The magnitudes of these parameters reflect three dominant effects: (i) the major changes in the degrees of freedom that occur when α -CD is threaded onto **S**, (ii) constraints placed on the movement of α -CD from one position to the next when threaded on **S**, and (iii) changes in hydration accompanying effects i and ii.

(33) For the first reaction step at 200 MPa, the observed rate constants were not determined over all the α -CD concentration range due to the reaction becoming too fast under such conditions for the high-pressure stopped-flow equipment (dead time 2 ms).

(34) Van Eldik, R.; Asano, T.; Le Noble, W. J. *Chem. Rev.* **1989**, *89*, 549.

Table 1. Thermodynamic and Kinetic Parameters for the Threading Reactions of α -CD by **S**

	NMR	stopped-flow	stopped-flow	
			ΔH (kJ mol ⁻¹)	ΔS (J K ⁻¹ mol ⁻¹)
$k_{1,f}^{298}$ (M ⁻¹ s ⁻¹)		15200 ± 200	$\Delta H_{1,f}^\ddagger = +23.5 \pm 0.7$	$\Delta S_{1,f}^\ddagger = -91 \pm 4$
$k_{1,r}^{298}$ (s ⁻¹)		4.4 ± 0.3	$\Delta H_{1,r}^\ddagger = +49.7 \pm 0.3$	$\Delta S_{1,r}^\ddagger = -67 \pm 13$
K_1^{298} (M ⁻¹)		3470 ± 250	$\Delta H_1^0 = -26.2 \pm 0.5$	$\Delta S_1^0 = -24 \pm 13$
K_1^{274} (M ⁻¹)	12600 ± 800 ^a	10300 ± 1500		
$k_{2,f}^{298}$ (M ⁻¹ s ⁻¹)		98 ± 2	$\Delta H_{2,f}^\ddagger = +36.7 \pm 1.0$	$\Delta S_{2,f}^\ddagger = -86 \pm 5$
$k_{2,r}^{298}$ (s ⁻¹)		0.032 ± 0.002	$\Delta H_{2,r}^\ddagger = +60.1 \pm 2.5$	$\Delta S_{2,r}^\ddagger = -76 \pm 9$
K_2^{298} (M ⁻¹)		3060 ± 190	$\Delta H_2^0 = -23.4 \pm 1.8$	$\Delta S_2^0 = -10 \pm 10$
K_2^{274} (M ⁻¹)	8800 ± 390 ^a	7690 ± 650		
$k_{3,f}^{298}$ (s ⁻¹)		0.158 ± 0.006	$\Delta H_{3,f}^\ddagger = +47.5 \pm 1.9$	$\Delta S_{3,f}^\ddagger = -96 \pm 7$
$k_{3,r}^{298}$ (s ⁻¹)		0.148 ± 0.006	$\Delta H_{3,r}^\ddagger = +59.6 \pm 2.0$	$\Delta S_{3,r}^\ddagger = -65 \pm 8$
K_3^{298}		1.07 ± 0.06	$\Delta H_3^0 = -12.1 \pm 1.9$	$\Delta S_3^0 = -31 \pm 10$
K_3^{274}	2.8 ± 0.1 ^a	1.9 ± 0.2		
$k_{4,f}^{298}$ (M ⁻¹ s ⁻¹)		9640 ± 1800 ^b	$\Delta H_{4,f}^\ddagger = +42.7 \pm 7.6$	$\Delta S_{4,f}^\ddagger = -31 \pm 27$
$k_{4,r}^{298}$ (s ⁻¹)		61 ± 6 ^b	$\Delta H_{4,r}^\ddagger = +78.7 \pm 4.0$	$\Delta S_{4,r}^\ddagger = +53 \pm 12$
K_4^{298} (M ⁻¹)		158 ± 14	$\Delta H_4^0 = -36.2 \pm 3.6$	$\Delta S_4^0 = -84 \pm 15$
K_4^{274} (M ⁻¹)	664 ± 28 ^a	710 ± 110		

^a Results from the NMR titration. ^b Results from variable-temperature NMR measurements: the dissociation rate constant, $k_{4,r}^{298}$, derives directly from the exchange analysis and the association rate constant, $k_{4,f}^{298}$, results from the multiplication of $k_{4,r}^{298}$ by the value of the equilibrium constant, K_4^{298} , obtained by stopped-flow measurements. The same procedure is applied for the determination of the enthalpies and entropies of activation.

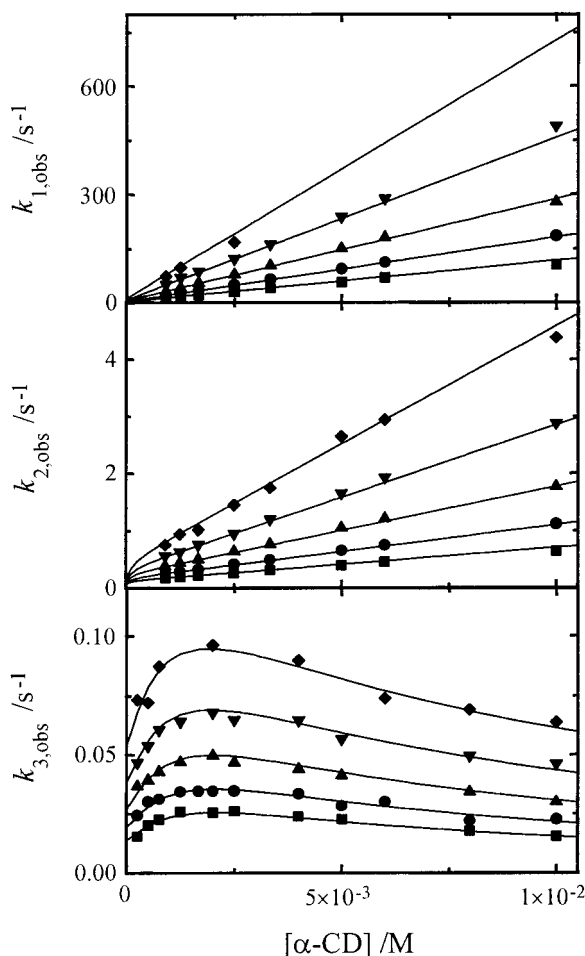


Figure 8. Pressure dependence of $k_{1,obs}$, $k_{2,obs}$, and $k_{3,obs}$ for the threading of α -CD by **S**: $C_S = (1.5\text{--}5.0) \times 10^{-5}$ M, $I = 0$ M, $T = 288$ K, and $P = 2$ (■), 50 (●), 100 (▲), 150 (▼), or 200 (◆) MPa.

The dye, **S**, exists as a dianion that is 2% dimerized ($K_{assoc} = 187$ M⁻¹) in a facile equilibrium under the conditions of the stopped-flow spectrophotometric studies.³⁵ It is assumed that the dimer is not involved in the threading process and that **S** exists as the trans isomer (Figure 1). No evidence was found for an equilibrium between the trans isomer and a cis isomer as discussed above.

Formation of S· α -CD*. It is known that the direction of binding is highly important in the reaction mechanism. The 3-carboxy-4-hydroxy-5-methylphenyl tail of **S** is too large to enter the α -CD cavity and consequently the sulfonate head enters the cavity through the wide end delineated by the 12 secondary hydroxy groups to form **S**· α -CD*. This orientation is in accord with that proposed for the threading of structurally similar but shorter dyes by α -CD.⁶ The formation of **S**· α -CD* is enthalpy-driven ($\Delta H_1^0 = -26.2$ kJ mol⁻¹) and characterized by $\Delta S_1^0 = -24$ J K⁻¹ mol⁻¹, which reflects the loss of degrees of freedom of the **S** and α -CD components. The rate constants of the first step, $k_{1,f}$ and $k_{1,r}$, are of the same order of magnitude as those reported for shorter but structural similar diazodiphenyl dyes that also thread α -CD, where $k_{1,f} \approx 12\,000\text{--}15\,000$ M⁻¹ s⁻¹ and $k_{1,r} \approx 2\text{--}25$ s⁻¹.⁶ It was shown that $k_{1,f}$ reflects the dehydration of the entering group and its interactions with bound water molecules inside the host cavity, whereas $k_{1,r}$ is dependent on the structure of the noninserting group. Our results are consistent with that conclusion and suggest that guest **S** is deeply inserted in the α -CD cavity, consistent with a small value for $k_{1,r}$.

The large negative activation entropy, $\Delta S_{1,f}^\ddagger = -91$ J K⁻¹ mol⁻¹, indicates a large loss of degrees of freedom associated with the combination of the single **S** and α -CD entities into a single transition state entity in which the sulfonate group retains some of its hydration shell while also interacting with water inside the α -CD cavity and the secondary hydroxy groups of the α -CD. This effectively locks the relative orientations of the **S** and α -CD transition-state components and adds to the loss of degrees of freedom. The dethreading process is also characterized by a large negative activation entropy, $\Delta S_{1,r}^\ddagger = -67$ J K⁻¹ mol⁻¹, and is consistent with the reversal of the approach to the transition state proposed for threading. The more negative values of $\Delta S_{1,f}^\ddagger$ and $\Delta S_{1,r}^\ddagger$ by comparison with that of ΔS^0 may indicate that in the **S**· α -CD* ground state α -CD rotates more freely about the **S** axis as a consequence of lesser steric and hydration constraints. While the enthalpic and entropic contributions to $\Delta G_{1,f}^\ddagger$ for the threading of α -CD are similar, the enthalpic term ($\Delta H_{1,r}^\ddagger = +49.7$ kJ mol⁻¹) for dethreading α -CD is twice the magnitude of threading ($\Delta H_{1,f}^\ddagger = +23.5$ kJ

(35) Since the pK_a of the phenol group and the carboxylic acid group of **S** are 11.51 and ≈ 2.5 , respectively, and application of 200 MPa induces a decrease in pK_a of ≈ 0.5 in water, the dianionic form of **S** persists as the only form of **S** in the high-pressure experiments.

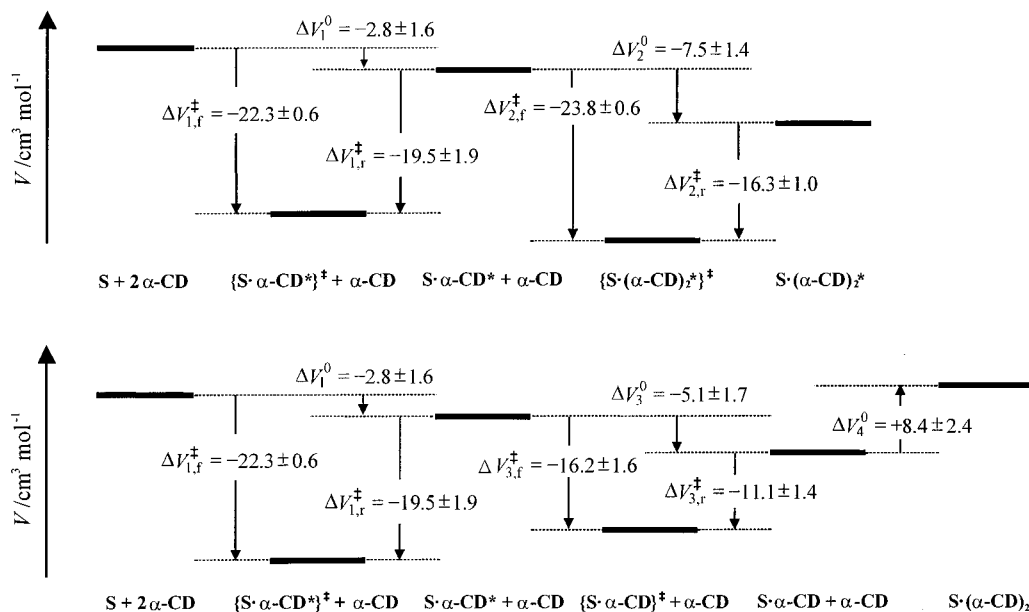


Figure 9. Volume profiles for the threading of α -CD by **S** at 288 K, in aqueous solution.

mol^{-1}). This is consistent with the dethreading process overcoming significant van der Waals forces between **S** and α -CD as the transition state is approached.

The volume profile for the formation of $\text{S} \cdot \alpha\text{-CD}^*$ shows the reaction volume, $\Delta V_1^0 = -2.8 \text{ cm}^3 \text{ mol}^{-1}$, to be small and consistent with the displacement of the water in the α -CD cavity by **S** and the sulfonate group being solvated largely as in the free state while retaining hydrogen-bonding interactions with α -CD primary hydroxy groups. In contrast, the activation volumes $\Delta V_{1,f}^\ddagger = -22.3 \text{ cm}^3 \text{ mol}^{-1}$ and $\Delta V_{1,r}^\ddagger = -19.5 \text{ cm}^3 \text{ mol}^{-1}$ are consistent with a substantial volume compression occurring on proceeding from the ground state to the transition state. Thus, in addition to a decrease in volume occurring as **S** enters the annulus, a decrease occurs as the sulfonate with much of its hydration shell intact enters the secondary end of α -CD, where it interacts with the water in the α -CD cavity and the secondary hydroxy groups to produce a substantial electrostriction.

Formation of $\text{S} \cdot (\alpha\text{-CD})_2^*$. The complex $\text{S} \cdot \alpha\text{-CD}^*$ first formed upon threading of α -CD by **S** can either isomerize to a second 1:1 complex $\text{S} \cdot \alpha\text{-CD}$ or thread an additional α -CD to form the 1:2 complex $\text{S} \cdot (\alpha\text{-CD})_2^*$. NMR structural studies of the latter pointed toward a head-to-tail orientation between the α -CD units and thus support the conclusion that the insertion mode of **S** in both cavities is similar. The stepwise stability constants and reaction enthalpies and entropies characterizing $\text{S} \cdot \alpha\text{-CD}^*$ and $\text{S} \cdot (\alpha\text{-CD})_2^*$ are identical within experimental error. This suggests that the forces stabilizing both complexes are similar and are dominated by van der Waals interactions between **S** and α -CD. However, the kinetics of the threading and dethreading of the first and second α -CDs differ significantly. Thus, the threading of the second α -CD onto **S** proceeds 150 times more slowly than the threading of the first α -CD because of a substantially increased activation enthalpy ($\Delta\Delta H^\ddagger = +13 \text{ kJ mol}^{-1}$). Similarly, the dethreading of the second α -CD occurs 140 times more slowly than that of the first α -CD because of a significant increase in the activation enthalpy ($\Delta\Delta H^\ddagger = +10 \text{ kJ mol}^{-1}$). However, the corresponding activation entropies of the threading and dethreading of the first and second α -CD are identical within experimental error and are consistent with similar changes in degrees of freedom. The

slowing of the threading and dethreading of the second α -CD indicates hindrance arising from the presence of the first α -CD. It is clear from this that an interaction between both α -CDs occurs in both threading and dethreading processes, but the extent and nature of this interaction cannot be precisely determined from the present data.

The volume of reaction, $\Delta V_2^0 = -7.5 \text{ cm}^3 \text{ mol}^{-1}$, is significantly more negative than ΔV_1^0 . Volume changes arising from the threading of the second α -CD are more likely to approximate those accompanying the threading of the first α -CD. Accordingly, it is probable that the greater magnitude of ΔV_2^0 is attributable to a conformational change in either one or both α -CDs. Such a volume change appears most readily achieved through reorientation of the flexible primary hydroxy arms units. As in $\text{S} \cdot (\alpha\text{-CD})_2^*$ the second α -CD occupies a similar position to α -CD in $\text{S} \cdot \alpha\text{-CD}^*$, it appears probable that the first α -CD is most likely to undergo such a conformational change possibly through a direct interaction with the second α -CD molecule. Both $\Delta V_{2,f}^\ddagger$ and $\Delta V_{2,r}^\ddagger$ are largely explicable as for $\Delta V_{1,f}^\ddagger$ and $\Delta V_{1,r}^\ddagger$.

Formation of $\text{S} \cdot \alpha\text{-CD}$. The isomeric equilibrium between $\text{S} \cdot \alpha\text{-CD}^*$ and $\text{S} \cdot \alpha\text{-CD}$ represents a molecular shuttling process^{36,37} where $K_3^{298} \approx 1$. The stabilities of both isomers are similar within the context of movement of α -CD between the two occupied sites on the **S** axis. Both $k_{3,f}$ and $k_{3,r}$ are smaller than $k_{1,r}$, and as a consequence the dethreading of α -CD occurs 30 times more frequently than the shuttling process at 298.2 K. The possibility exists that the conformation of **S** may be significant in determining the rate of the shuttling process. The three phenyl groups are drawn in a coplanar orientation in Figure 1, as expected for **S** in the uncomplexed state.³⁸ It is known that rotation out of the common plane of one or more of the phenyl and naphthalene groups of structurally similar Congo Red occurs depending upon environment,^{39,40} and it is possible that a similar rotation about the C–N bonds may be significant

(36) Kawaguchi, Y.; Harada, A. *Org. Lett.* **2000**, 2, 1353.

(37) Lane, A. S.; Leigh, D. A.; Murphy, A. *J. Am. Chem. Soc.* **1997**, 119, 9, 11092 and references therein.

(38) Gilardi, R. D.; Karle, I. L. *Acta Crystallogr., Sect. B* **1972**, 28, 1635.

(39) Turnel, W. G.; Finch, J. T. *J. Mol. Biol.* **1992**, 227, 1205.

(40) Ojala, W. H.; Ojala, C. R.; Gleason, W. B. *Antiviral Chem. Chemother.* **1995**, 6, 25.

in determining the thermodynamics of the shuttling process in $\mathbf{S}\cdot\alpha\text{-CD}^*$ and $\mathbf{S}\cdot\alpha\text{-CD}$.

Together ΔS_3^0 and ΔV_3^0 are consistent with a loss of degrees of freedom and a contraction of volume on formation of $\mathbf{S}\cdot\alpha\text{-CD}$ which most probably reflects conformational changes in $\alpha\text{-CD}$ and possibly in \mathbf{S} . The large negative $\Delta S_{3,f}^\ddagger$, $\Delta S_{3,r}^\ddagger$, $\Delta V_{3,f}^\ddagger$ and $\Delta V_{3,r}^\ddagger$ are internally self-consistent as they simultaneously indicate losses of degrees of freedom and contraction in volume in forming the transition state. Once again, conformational changes in both $\alpha\text{-CD}$ and \mathbf{S} appear a plausible source of these observations, together with changes in the electrostriction of water at the transition state.

Formation of $\mathbf{S}\cdot(\alpha\text{-CD})_2$. At 298.2 K, the threading of a second $\alpha\text{-CD}$ onto $\mathbf{S}\cdot\alpha\text{-CD}$ ($k_{4,f} \approx 9460 \text{ M}^{-1} \text{ s}^{-1}$) is substantially faster than in the threading of a second $\alpha\text{-CD}$ onto $\mathbf{S}\cdot\alpha\text{-CD}^*$ ($k_{2,f} \approx 98 \text{ M}^{-1} \text{ s}^{-1}$). This is consistent with a lesser degree of steric hindrance characterizing the threading of the second $\alpha\text{-CD}$ onto $\mathbf{S}\cdot\alpha\text{-CD}$ because the first $\alpha\text{-CD}$ is more distant from the sulfonate head of \mathbf{S} than is the case for $\mathbf{S}\cdot\alpha\text{-CD}^*$. The dethreading of $\alpha\text{-CD}$ from $\mathbf{S}\cdot(\alpha\text{-CD})_2$ is also much faster than in the case of $\mathbf{S}\cdot(\alpha\text{-CD})_2^*$, but it is $\mathbf{S}\cdot(\alpha\text{-CD})_2^*$ that is the substantially more stable complex, as a consequence of ΔS_2^0 being much less negative than ΔS_4^0 . On a structural basis the lower stability of $\mathbf{S}\cdot(\alpha\text{-CD})_2$ may be attributable to both $\alpha\text{-CD}$ s being threaded less deeply than is the case for $\mathbf{S}\cdot(\alpha\text{-CD})_2^*$. Because of its lower stability, $\mathbf{S}\cdot(\alpha\text{-CD})_2$ is formed in a low concentration, thus making the structure determination by NMR difficult. However, the threading of the second $\alpha\text{-CD}$ onto $\mathbf{S}\cdot\alpha\text{-CD}$ probably involves the entry of the sulfonate head through the wide rim of $\alpha\text{-CD}$ as for the other threading processes of the present study. This conclusion is based on the lesser steric hindrance toward sulfonate entry through the wide rim, which is more hydrophilic by comparison with the narrow rim, which is more hydrophobic.⁴¹

Although the errors in the activation parameters are large, there is a clear trend for $\Delta H_{4,f}^\ddagger$ and $\Delta H_{4,r}^\ddagger$ to be larger than $\Delta H_{2,f}^\ddagger$ and $\Delta H_{2,r}^\ddagger$ and for $\Delta S_{4,f}^\ddagger$ and $\Delta S_{4,r}^\ddagger$ to be less negative than $\Delta S_{2,f}^\ddagger$ and $\Delta S_{2,r}^\ddagger$. The positive reaction volume, $\Delta V_4^0 = +8.4 \text{ cm}^3 \text{ mol}^{-1}$, contrasts with $\Delta V_2^0 = -7.5 \text{ cm}^3 \text{ mol}^{-1}$ and suggests substantial differences in the contributions made by hydrational, conformational, and van der Waals interactions to the volume changes and energetics of the formation of $\mathbf{S}\cdot(\alpha\text{-CD})_2$ and $\mathbf{S}\cdot(\alpha\text{-CD})_2^*$. There are three probable origins of these differences. The first is that the hydration of the sulfonate group may be less significant for the complex $\mathbf{S}\cdot(\alpha\text{-CD})_2$, where the second $\alpha\text{-CD}$ is closer to the sulfonate head of \mathbf{S} . The second

is that in one complex the two $\alpha\text{-CD}$ s may act largely as a single unit as a consequence of hydrogen bonding between them,^{42,43} whereas this may be less significant in the other complex. The third is that twisting of phenyl groups of \mathbf{S} out of a common plane may occur to a greater extent in one complex than the other and thereby contribute to the differences in observed enthalpic, entropic, and volume change differences between the two complexes. Unfortunately, insufficient structural data is available to ascertain the veracity of these proposals. However, it is very probable that the origins of these differences between $\mathbf{S}\cdot(\alpha\text{-CD})_2$ and $\mathbf{S}\cdot(\alpha\text{-CD})_2^*$ are also the origins of the nonobservation of a direct exchange path between them so that an indirect interchange occurs through the dethreading of $\alpha\text{-CD}$ and shuttling of $\alpha\text{-CD}$ in $\mathbf{S}\cdot\alpha\text{-CD}$ and $\mathbf{S}\cdot\alpha\text{-CD}^*$.

Conclusion

In this first kinetic high-pressure study of the sequential threading of $\alpha\text{-CD}$ onto a dye guest molecule, \mathbf{S} , it has been found that the structure of \mathbf{S} is important in determining the position of the threaded $\alpha\text{-CD}$ s and the stability and kinetics of threading and dethreading. Two isomeric 1:1 complexes, $\mathbf{S}\cdot\alpha\text{-CD}^*$ and $\mathbf{S}\cdot\alpha\text{-CD}$, are formed, where in the second complex \mathbf{S} is more deeply imbedded in $\alpha\text{-CD}$ than in the first. Both $\mathbf{S}\cdot\alpha\text{-CD}^*$ and $\mathbf{S}\cdot\alpha\text{-CD}$ thread a second $\alpha\text{-CD}$ to form 1:2 complexes, $\mathbf{S}\cdot(\alpha\text{-CD})_2^*$ and $\mathbf{S}\cdot(\alpha\text{-CD})_2$, but these isomeric complexes do not directly interconvert. Instead, they both dethread one $\alpha\text{-CD}$ to form either $\mathbf{S}\cdot\alpha\text{-CD}^*$ or $\mathbf{S}\cdot\alpha\text{-CD}$, which then isomerize prior to threading a second $\alpha\text{-CD}$ to re-form $\mathbf{S}\cdot(\alpha\text{-CD})_2^*$ and $\mathbf{S}\cdot(\alpha\text{-CD})_2$. The quantitative ground-state and activation enthalpy, entropy, and volume change studies show that hydrational, van der Waals, and probably conformational changes in \mathbf{S} and $\alpha\text{-CD}$ determine the equilibrium and kinetic character of the system.

Acknowledgment. The Swiss National Science Foundation is greatly thanked for financial support. We also wish to thank Fabrice Yerly for his help in the preparation of the figures and for the fit of the data, and Pascal Fuchsman for the purification of the dye.

Supporting Information Available: Four tables containing stopped-flow kinetic data; four figures showing $\pi\text{-}\pi$ stacking NMR data, a 2D ^1H ROESY spectrum of the 1:2 complexes, and ^1H NMR fast injection and exchange experiments; and derivation of the kinetic equations (PDF). This material is available free of charge via the Internet at <http://pubs.acs.org>.

JA010946O

(42) Bonnet, P.; Jaime, C.; Morin-Allory, L. *J. Org. Chem.* **2001**, *66*, 689.

(43) Harata, K. *Chem. Rev.* **1998**, *98*, 1803 and references therein.

(41) Lipkowitz, K. B. *Chem. Rev.* **1998**, *98*, 1829.